Intramolecular Electronic Redistribution Coupled to Hydrogen Bonding: An Important Mechanism for the "Neutral-to-Ionic" Transition

Vincent Oison,* Claudine Katan, and Christiane Koenig

Groupe Matière Condensée et Matériaux (UMR CNRS 6626), Université Rennes I, Campus de Beaulieu, F-35042 Rennes Cedex, France

Received: September 21, 2000

The part played by the electronic interactions in the uncommon "neutral-to-ionic" (N-I) structural transition occurring in some mixed stack organic compounds, such as tetrathiafulvalene-chloranil (TTF-CA), is analyzed by ab initio electronic structure calculations. It is shown that the charge-transfer variation occurring in the valence band along the mixed stacks of donor and acceptor molecules is coupled via an intramolecular mechanism to a deformation of the electronic cloud in lower bands. The lower bands affected by this redistribution are also those which are implicated in the interstack hydrogen bonds, and a charge-transfer increase produces a strengthening of these hydrogen bonds. This important mechanism, which associates the charge-transfer variation to the anisotropic lattice contractions in the crystal, has never been considered up to now.

I. Introduction

Organic molecular compounds often present very interesting one-dimensional (1D) or two-dimensional (2D) physical properties, due to the existence of molecular stacks or sheets in the crystalline structure. By modifying slightly the stacking in the crystal, external pertubations such as pressure or temperature induce drastic variations of these properties. A good illustration is offered by the series of mixed stack charge-transfer (CT) salts formed with the well-known donor (D) molecules TTF, DMTTF, etc. and acceptor (A) molecules, for example, benzoquinone derivatives (Figure 1). Several compounds of this series undergo a structural phase transition characterized at high pressure or low temperature by the loss of inversion symmetry; for a few of them, classified as "neutral-to-ionic" (N-I) compounds such as TTF-CA,[1] TTF-2,5Cl_2BQ,[2] and DMTTF-CA,[3] this transition is accompanied by a large and sometimes discontinuous variation of the CT from D to A (of the order of 0.4 e in TTF-CA). In these uncommon ferro- or antiferroelectric transitions, the macroscopic electric polarization in the low-symmetry phase arises both from the displacement of the atoms and from their charge variation.

Due to the existence of mixed stacks of D and A molecules in these semiconductors and to the strong anisotropy of their optical and transport properties,[4] effective 1D models built with hopping integrals along the stacks between the frontier molecular orbitals have been proposed to describe the competition between electronic and dynamical mechanisms at the origin of these peculiar transitions.[5,6] However, these models are not specific enough to predict the different features of these compounds, nor to explain why other mixed stack compounds such as TTF-BA[7] do not undergo such transitions. These models ignore any quantum interstack interactions despite a clear indication in the experimental structural data of very different and sometimes short intermolecular distances in these crystals.[8,9] In particular, the existence of a three-dimensional (3D) network of hydrogen bonds related to the anisotropic lattice contractions in TTF-CA has been underlined a long time ago.[9]

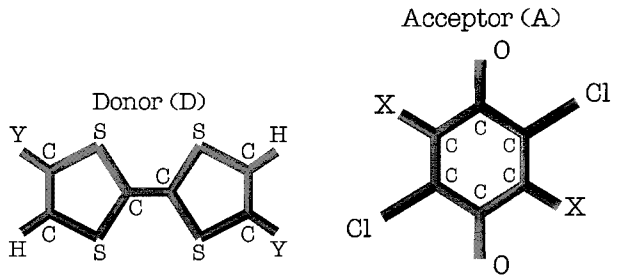

Figure 1. Backbone of D and A molecules: Y = H for TTF, Y = CH_3 for DMTTF, X = Cl for CA, X = H for TTF-2,5Cl_2BQ.

On the other hand, ab initio self-consistent numerical techniques offer nowadays a unique tool for analyzing the electronic structure of these compounds, without any beforehand assumption concerning the relative strengths of the intermolecular interactions. Our aim is to analyze the electronic reorganization associated to the structural transition, and estimate the part played, respectively, by the different intra- and interstack molecular bonds in the CT variation and the lattice contractions. Our work is based on the three compounds TTF-2,5Cl_2BQ, TTF-CA and DMTTF-CA, for which recent structural data[8,10] together with an extended study of the physical properties under temperature and pressure variations are available. Ab initio calculations in the crystals[11,12] allow the visualization, in each energy band, of the nature of the electronic states involved in the formation of molecular chains and sheets in the crystal. The intermolecular interactions responsible for these crystalline structures can then be analyzed in terms of couplings between molecular orbitals (MO) of the D and A molecules (section III). Going beyond the limitation to frontier orbitals, we first analyze in section IV the intramolecular electronic redistribution of deep MO's due to a variation of population in the frontier MO's, by ab initio calculations on isolated and charged molecules. Section V emphazises the role of those deep deformations on the strength of the interstack local contacts, especially in the

* Corresponding author. Fax: 33 2 99 28 67 17. E-mail: Vincent.Oison@univ-rennes1.fr.

10.1021/jp003425g CCC: $20.00
Published on Web 04/05/2001

directions of marked lattice contractions, as observed in TTF-CA.[12] The short D−A interchain hydrogen bonds existing in these compounds are reproduced by considering an isolated complex A−D−A of three coplanar molecules coupled by hydrogen bonds. Our calculations reveal an important coupling between CT variations and lateral lattice contractions, which has never been considered up to now. The implications of this coupling for the N-I transition are discussed in the last section.

II. Computational Details

All electronic structure calculations and atomic relaxations have been performed with the projector augmented wave (PAW) method.[13] This method combines the original fictitious Lagrangian approach of Car and Parrinello,[14] in which the atomic coordinates and the electronic wave function are treated simultaneously by a set of Newton's equations, with an efficient all-electron electronic structure scheme. Our calculations are based on the density functional theory within the local density approximation (LDA). We have used the LDA parametrization by Perdew and Zunger[15] based on Monte Carlo simulations of the free electron gas by Ceperley and Adler,[16] Becke's gradient corrections to the exchange energy,[17] and Perdew's gradient correction to the correlation energy.[18] These gradient corrections to the LDA are known to be well adapted when hydrogen bonds are involved.[19] In sections IV and V, concerning isolated molecules or complexes, the pseudo-wave functions were expanded into plane waves up to a kinetic energy cutoff of 35 Ry and the density up to 140 Ry. The calculations were carried out using supercells, the molecules being electrostatically decoupled from their periodic images.[20] Convergence with respect to the kinetic energy cutoff and supercell size has been verified.

III. Crystalline Structure and Charge Transfer

We have already performed ab initio calculations of the electronic structure of TTF-2,5Cl_2BQ and TTF-CA[11,12] in their high-symmetry (HS) and low-symmetry (LS) phases. These calculations provide the self-consistent electron density $n(\vec{r})$ in real space, allowing thus to check the dimensionality of this density and to identify the nature of the electronic states responsible for the packing of the crystals. As the molecules remain nearly flat even in the LS phase, this density can be locally separated in π and σ contributions with respect to the molecular planes. It is also possible to isolate the contribution $n_{VB}(\vec{r})$ of the valence band (VB) from the one of lower bands (LB).

The first structural characteristic of these compounds is the existence of mixed chains (Figure 2) of D and A molecules along a crystallographic direction which is noted[21] $\vec{a}_1$. Our calculations have confirmed that $n_{VB}(\vec{r})$ is to some extent delocalized along these chains and can be interpreted as resulting from hybridization between the highest occupied molecular orbital (HOMO) of D and the lowest unoccupied molecular orbital (LUMO) of A, both of π character but with different symmetries.[12] These two MO's and the existence of mixed chains, which we will call "π chains", are at the basis of the two-band and 1D models developed up to now to describe the phase transitions in this series of compounds.[6]

But it has also been known for a long time that other intermolecular contacts, especially a 3D network of hydrogen bonds,[9] play a role in the crystal structure and its transformations. The strongest O···H interactions occur along mixed chains of coplanar D and A molecules in the direction[21] $\vec{a}_2 + \vec{a}_1/2$, which we will call "OH chains" (Figure 2). Our calculations

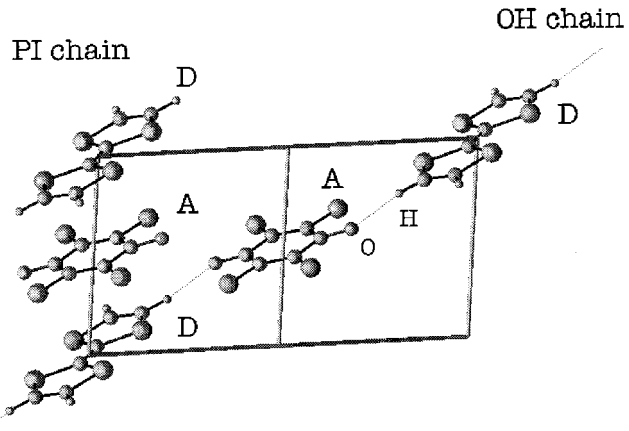

Figure 2. Representation of a π chain (// $\vec{a}_1$) and an OH chain (// $\vec{a}_1/2 + \vec{a}_2$).

have shown that $n(\vec{r})$ is of the same order of magnitude between D and A molecules along the OH chains as along the π chains, and that the OH contacts are essentially made of deep MO's of σ character. The configuration in π and OH chains is a specificity of this series: the intersecting axes of these chains form very similar crystallographic planes[12] ($\vec{a}_1$, $\vec{a}_2$) in the three compounds considered here. In the third direction, $\vec{a}_3$, the intermolecular interactions and structural configurations are very different from one compound to the other. This may be partly at the origin of the observed different behaviors of these compounds.

Although the CT is not a well-defined concept, the estimate of its variation should be attempted, as it is one of the most stricking aspects of these structural transitions. The experimental determination of the CT often relies on the linear variation of some intramolecular bond lengths or vibrational frequencies with respect to the molecular charge.[1,2] It thus carries an intrinsic deficiency due to the transfer of molecular properties from one crystalline environment to an other one. From the theoretical point of view, the situation is not better, the numerical value of this CT being strongly model dependent.[22] In two-band tight-binding Hamiltonians based on linear combinations of the HOMO of D and the LUMO of A, the hybridization with deeper MO's is neglected. The CT is given by the mean value in the Brillouin zone of the weight of the LUMO of A in the Bloch function of the VB. In this model fitted to our ab initio calculations, we have obtained for TTF-2,5Cl_2BQ in its HS phase a CT of the order of 0.4 e,[12] not far from the experimental value of 0.3 e. However, it is most likely that the contribution from LB's to the CT is non-negligible especially from bands involved in the interchain contacts. In the N-I transition, the increase of the CT in the valence band is directly related to the contraction along the π chains and to the loss of inversion symmetry, which allows a hybridization between the HOMO of D and the LUMO of A at the center of the Brillouin zone.[12,23] On the other hand, at the transition in TTF-CA, neutron measurements[8,10] have put in evidence a marked contraction of the OH bond lengths and a discontinuous variation of $\vec{a}_2$ related to the discontinuity of the CT. So, it is obvious that in the mechanism of the N-I transition an important coupling exists between some low-lying electronic states implicated in the OH bonds and lateral lattice contractions and the valence states responsible for the essential part of the charge transfer. Our aim is to analyze its importance and implications by ab initio calculations in isolated molecules and complexes.

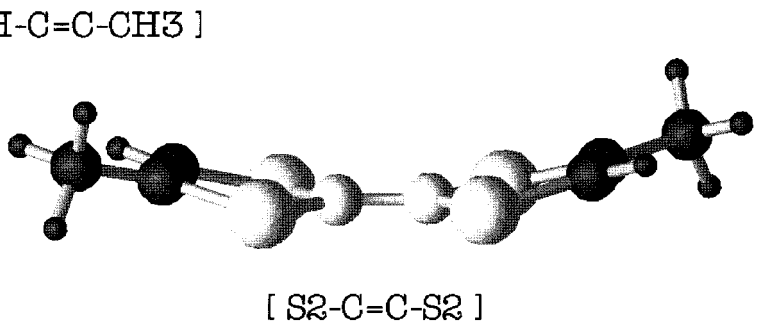

Figure 3. Boatlike structure of DMTTF.

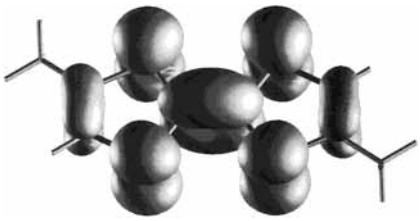

Figure 4. Isodensity representation ($n(\vec{r}) = 0.002\ e^-/\text{au}^3$) of the HOMO of the DMTTF molecule. The HOMO has no weight on H and CH_3.

IV. Isolated and Charged Molecules

To analyze the interactions between frontier and lower MO's in a charged molecule $D^{+\rho}$ or $A^{-\rho}$, we have performed ab initio calculations of its electronic structure by the PAW method.[13] For each value of the charge, we have obtained the equilibrium geometry by relaxing the atomic positions. The effect of the charge is 2-fold.

A. Geometrical Deformations and Global Properties. Our results for TTF[24] and CA[25] have already been published. As expected, the behavior of DMTTF is very similar to the one of TTF. The neutral molecule has two stable configurations with nearly equivalent total energies: a flat structure (apart from CH_3) of C_{2h} symmetry and a boatlike structure in which the fragments [$CH_3C-C{=}C-H$] are bent with respect to the central fragment [$S_2-C{=}C-S_2$] (Figure 3, see also Figure 1) with an angle of about 15°. As the charged molecule, as well as charged TTF and CA, is flat and remains nearly flat in the crystal, we consider only flat molecules in the following. In DMTTF, the central C=C and C−S bond length display, respectively, a linear increase (3% for $\rho = 1$) or decrease (2%) versus charge variation, which can be understood from the respective bonding and antibonding character of these bonds in the HOMO of the molecule (Figure 4).

From a series expansion of the total energy E of a molecule carrying a charge $\rho = \rho\downarrow + \rho\uparrow$ on its frontier orbital of energy ϵ_0[26]

$$E(\rho\downarrow,\rho\uparrow) = E(0,0) + \epsilon_0(\rho\downarrow + \rho\uparrow) + \frac{1}{2}U(\rho\downarrow + \rho\uparrow)^2 - \frac{1}{2}J(\rho\downarrow + \rho\uparrow)^2 \quad (1)$$

the Coulomb U and exchange J energies can be deduced, as well as the ionization energy I, which are used as parameters in model Hamiltonians. For DMTTF, we obtain $\epsilon_0 = -3.90$ eV (energy of the HOMO), $U = 4.30$ eV, and $J = 0.18$ eV, values which are not far from those found previously for TTF,[24] and $I = 6.04$ eV, very near its experimental value of 6.1 eV.[27]

B. Electronic Redistribution and Chemical Reactivity. We analyze here the internal electronic redistribution $\Delta n(\vec{r})$ due to a charge $\rho = \pm 1e^-$ placed on the frontier MO of an isolated molecule in the fixed geometry of the flat neutral molecule (the consequences of the very small deformations of its backbone with charge are quite negligible here). In a finite difference approximation, this corresponds to the Fukui function[28,29] currently used in quantum chemistry. The effect of the charge being roughly linear, the redistribution for a fractional charge variation $\Delta\rho$ can then be deduced by simple scaling.

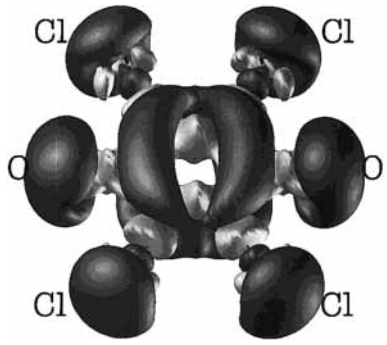

Figure 5. Isodensity representation of $\Delta n(\vec{r})$ for CA: dark (bright) isosurface corresponds to a gain (loss) of 0.001 e^-/au^3.

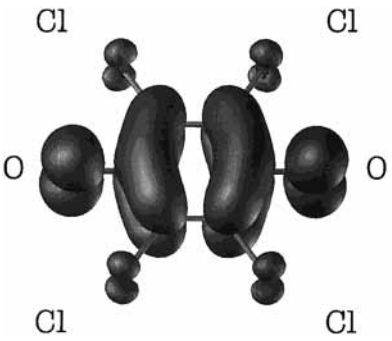

Figure 6. Isodensity representation ($n^-_{\text{LUMO}}(\vec{r}) = 0.002\ e^-/\text{au}^3$) of the LUMO ($\pi$ symmetry) of the CA molecule.

The addition of one electron in the LUMO of CA induces a global electronic variation (Figure 5)

$$\Delta n(\vec{r}) = n^-(\vec{r}) - n^0(\vec{r}) \quad (2)$$

where $n^-(\vec{r})$ and $n^0(\vec{r})$ are, respectively, the electron densities of CA^- and CA^0. $\Delta n(\vec{r})$ can be separated in two terms:

- the new density $n^-_{\text{LUMO}}(\vec{r})$ of π type (Figure 6), which carries the additional charge $\rho = 1e^-$ and has the same spatial shape as the empty LUMO of the neutral molecule, with no weight in the molecular plane.
- an induced spatial deformation or polarization of the lower MO's (LMO)

$$\Delta n_{\text{LMO}}(\vec{r}) = \Delta n(\vec{r}) - n^-_{\text{LUMO}}(\vec{r}) \quad (3)$$

This latter deformation is maximum in the molecular plane

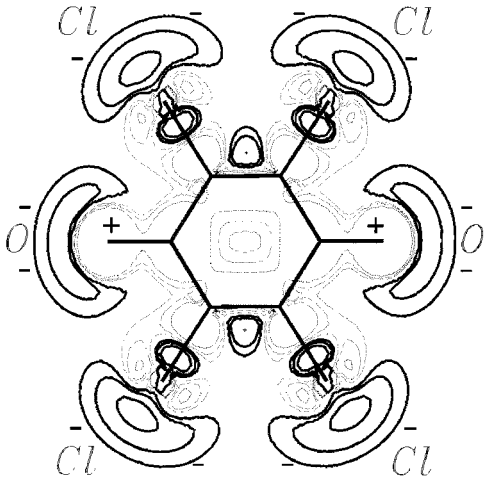

Figure 7. Isodensity curves of $\Delta n_{LMO}(\vec{r})$ in the plane of the CA molecule for ± 0.0005 e^-/au^3, ± 0.001 e^-/au^3, and ± 0.002 e^-/au^3.

TABLE 1: Atomic Charge Variations (in electron) for the Isolated CA Molecule

atom *i*	C(Cl)	C(O)	Cl	O
$\Delta q_i = q_i^{CA^-} - q_i^{CA^0}$	+0.01	−0.09	−0.14	−0.15

(Figure 7), which means that it is essentially of σ character. There are only a few π MO's below the LUMO (8 π compared to 24 σ); their deformations are weak and concealed behind the density variation in the LUMO, which dominates the π redistribution. The detailed analysis of the σ redistribution shows that it is principally due to the deformation of a few σ MO's, situated as far as 5 to 10 eV below the LUMO, and characterized by a non-negligible weight on Cl and O. This deformation is due to the electron−electron Coulomb and exchange−correlation interactions which couple all the MO's in the molecular Hamiltonian. In a self-consistent procedure, the increase of the population of the LUMO in a region of space (around C and O) acts as a repulsive potential on the electronic states of the other MO's in the same region.

This mechanism is especially efficient in some large σ MO's which have the possibility to accommodate on the periphery of the molecule (outside Cl and O) those of their electronic states which are expelled from the region occupied by the additional charge. The global result is a dilatation of the σ electronic cloud in the molecular plane. Atomic charges can be deduced from a set of Gaussian equations centered on the atoms and fitted so as to reproduce the successive multipolar moments of the total electron density.[20] Applied to CA^0 and CA^-, this leads to the atomic charge variations of Table 1. The gain of 0.15 e on each oxygen is essentially due to the occupation of the LUMO (Figure 6). Despite the weak weight of the LUMO on Cl, a gain of the same order is observed on these atoms: the LUMO occupation on the C atoms is partly compensated by a loss of σ states on these atoms to the benefit of the Cl atoms. The accumulation of negative charge outside the external atoms (Cl and O), visible in Figure 7, leads to an enhancement of the multipolar moments on these atoms. The increase of negative charge on this type of flat acceptor molecule results in an increase of the chemical reactivity of the molecule, especially in its plane.

The subtraction of one electron from the donor (TTF or DMTTF) has exactly the reverse effect. The total electronic redistribution in TTF,

$$\Delta n(\vec{r}) = n^+(\vec{r}) - n^0(\vec{r}) \tag{4}$$

where $n^+(\vec{r})$ and $n^0(\vec{r})$ are, respectively, the electron densities

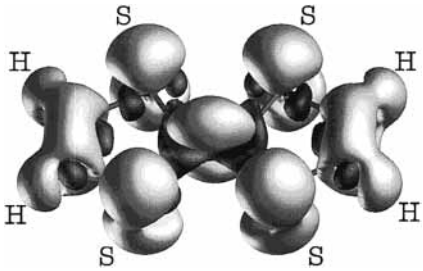

Figure 8. Isodensity representation of $\Delta n(\vec{r})$ for TTF: dark (bright) isosurface corresponds to a gain (loss) of 0.001 e^-/au^3.

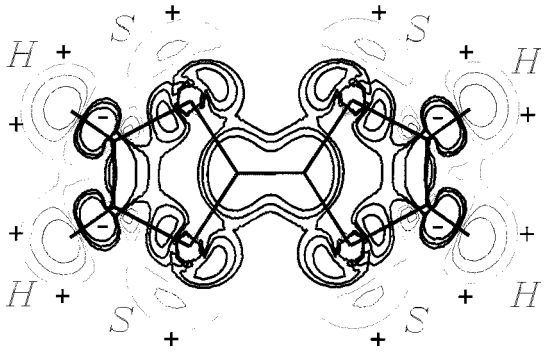

Figure 9. Isodensity curves of $\Delta n_{LMO}(\vec{r})$ in the plane of the TTF molecule for ± 0.0005 e^-/au^3, ± 0.001 e^-/au^3, and ± 0.002 e^-/au^3.

TABLE 2: Atomic Charge Variations (in electron) for the Isolated TTF Molecule

atom *i*	central C	S	C	H or CH_3
$\Delta q_i = q_i^{TTF^+} - q_i^{TTF^0}$	−0.04	+0.2	−0.03	+0.1

of TTF^+ and TTF^0, is displayed in Figure 8 where the depletion of the π states in the HOMO on the C and S atoms is clearly seen. Figure 9 represents the deformations of lower MO's in the molecular plane:

$$\Delta n_{LMO}(\vec{r}) = n^+_{LMO}(\vec{r}) - n^0_{LMO}(\vec{r}) \tag{5}$$

These deformations occur in a few deep σ MO's which have a non-negligible weight on H (on H and CH_3 in DMTTF). This produces an important polarization on these atoms and leads to an atomic point charge variation as large as 0.1 e on each H (Table 2). These latter atomic states are attracted toward the C atoms by the depletion of the HOMO, which they partly compensate in the total charge variation. The charge variation in the HOMO induces thus a contraction of the σ contribution to the electronic cloud, leaving an excess of positive charge on the periphery of the molecule, inducing important atomic moments, especially dipoles on the hydrogen atoms.

These two reverse effects are particularly interesting for N-I compounds where coplanar D and A molecules alternate along the OH chains. A CT from D to A, occurring via the interactions between the frontier orbitals along the π chains, is necessarily accompanied by an increase of opposite charges and nearly parallel dipoles on the two atoms O and H implicated in the hydrogen bonds. The resulting strengthening of these hydrogen bonds is studied in the next section in an isolated planar complex of A−D−A type.

V. TTF(H_2C=O)$_2$ Complex and Hydrogen Bond

We represent here the intermolecular contacts along the OH chains by considering an isolated planar and neutral complex of symmetry C_{2h}, formed with one TTF molecule coupled via

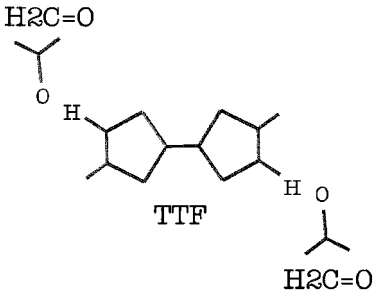

Figure 10. Structure of the TTF($H_2C{=}O)_2$ complex.

hydrogen bonds to two acceptors (Figure 10). To reduce the computational effort and simplify the analysis of the interacting states, we replace here the two CA molecules by two smaller acceptors. The choice for these acceptors should satisfy two requirements: they must have a C═O double bond with C in an sp^2 configuration and must also be equivalent to one-half of an A molecule in order to respect the stoichiometry. $H_2C{=}O$ seems to be the best candidate: to each MO of $H_2C{=}O$ corresponds one of CA; for the MO's of $H_2C{=}O$ with no weight on H (respectively on Cl in CA) this correspondence is very good, for the electronic density around C═O as well as for the energies. The complex is built so as to reproduce the atomic positions and angles around the hydrogen bond in the HS structure of TTF-CA, with an O−H distance of 2.34 Å. The TTF molecule considered here is in the optimized flat geometry of its neutral state. We have verified that the use of the actual backbone of TTF in the crystal TTF-CA does not modify our conclusions.

A. MO's of the TTF($H_2C{=}O)_2$ Complex. The first step is to analyze the mutual influence of the neutral fragments in the electronic states of the complex. The HOMO and LUMO of the complex are of π character and consist, respectively, in the HOMO of TTF and the LUMO of the $(H_2C{=}O)_2$ fragment, reproducing thus the configuration of the frontier MO's in the crystal, which is a fundamental requirement for the validity of our model. Among the 37 other occupied MO's of this complex, eight among the highest ones are of π character (with no weight on H) and are very similar to the π MO's of either fragment. The nine lowest MO's are deep σ MO's of the individual fragments. The cohesion of the complex compared to separate neutral fragments arises from intermediate σ MO's situated 5 to 10 eV below the HOMO, and more than 10 eV above the lowest one. More precisely, nine of these intermediate MO's result from nonnegligible hybridization between five σ MO's of TTF and four σ MO's of $(H_2C{=}O)_2$. Figure 11 displays one example of such a coupling.

It is important to note that the σ MO's of isolated fragments responsible for these hybridizations are precisely those which present a maximum deformation when the corresponding isolated molecules are charged (section IV). The resulting electronic redistribution compared to isolated neutral fragments

$$\Delta n_{\mathrm{P}}(\vec{r}) = n_{\mathrm{TTF}(H_2C=O)_2}(\vec{r}) - n^0_{\mathrm{TTF}}(\vec{r}) - n^0_{(H_2C=O)_2}(\vec{r}) \quad (6)$$

is displayed in Figure 12 in the molecular plane: it shows a clear polarization of the electronic cloud around the hydrogen bond, with formation of nearly parallel dipolar moments on H and O, which is a well-known signature of hydrogen bonding, and is responsible for the stabilization of the complex. The ab initio value of the cohesion energy of the complex is of about −5 kJ/mol, which is weak but of the order of magnitude expected for this kind of hydrogen contact.[30] We verified that the fragments remain globally neutral in the complex and that the Coulomb interactions between atomic point charges play a negligible role in the cohesive energy, which arises principally from the polarization of the electronic cloud along the hydrogen bonds.

B. Hydrogen Bond and Charge Transfer. In the "neutral" HS phase of the three compounds considered here, the CT is of about 0.3 e. This situation can be reproduced in the TTF-$(H_2C{=}O)_2$ complex by a transfer of 0.3 e from its HOMO to its LUMO, forming thus an "excited" but still neutral complex [TTF$(H_2C{=}O)_2$]*, each $H_2C{=}O$ representing half a CA molecule with a charge of 0.15 e. The global electronic redistribution compared to the neutral fragments

$$\Delta n^*(\vec{r}) = n_{[\mathrm{TTF}(H_2C=O)_2]^*}(\vec{r}) - n^0_{\mathrm{TTF}}(\vec{r}) - n^0_{(H_2C=O)_2}(\vec{r}) \quad (7)$$

is displayed in Figure 13 where the HOMO of TTF and the LUMO of $(H_2C{=}O)_2$ implicated in the CT are easily recognizable. In the plane of the complex (Figure 14) this deformation is essentially due to some lower MO's of σ type and can be analyzed in two terms:

• An internal redistribution in each fragment, due to the charge variation $\pm\rho$ on its frontier orbital

$$\Delta n^*_{\mathrm{F}}(\vec{r}) = (n^{+0.3}_{\mathrm{TTF}}(\vec{r}) - n^0_{\mathrm{TTF}}(\vec{r})) + (n^{-0.3}_{(H_2C=O)_2}(\vec{r}) - n^0_{(H_2C=O)_2}(\vec{r})) \quad (8)$$

We have shown in the previous section that this amounts to a dilatation or a contraction of the electronic cloud, leaving a net charge of same sign on the periphery of each fragment, and additional dipoles on H and O.

• A polarization of this cloud, only due to the mutual influence of the charged fragments

$$\Delta n^*_{\mathrm{P}}(\vec{r}) = n_{[\mathrm{TTF}(H_2C=O)_2]^*}(\vec{r}) - n^{+0.3}_{\mathrm{TTF}}(\vec{r}) - n^{-0.3}_{(H_2C=O)_2}(\vec{r}) \quad (9)$$

$\Delta n^*_{\mathrm{P}}(\vec{r})$ (Figure 15) displays a strengthening of the hydrogen bond, compared to the TTF$(H_2C{=}O)_2$ complex (Figure 12). This strengthening, only due to the charge transfer, is isolated in Figure 16, displaying $\Delta n^*_{\mathrm{P}}(\vec{r}) - \Delta n_{\mathrm{P}}(\vec{r})$. It arises from an increase of positive and negative charges, respectively, ahead of the H and O atoms, yielding a further enhancement of the dipolar moments on these atoms. In our ab initio calculations, the stabilization energy of the excited complex [TTF$(H_2C{=}O)_2$]* compared to isolated and charged fragments is −43 kJ/mol, 1 order of magnitude larger than in the TTF$(H_2C{=}O)_2$ complex. However, the part of this energy ascribable to point charges localized on the atoms is only of the order of −10 kJ/mol, so that its largest contribution (∼−30 kJ/mol) arises from distributed multipolar interactions, especially between the enhanced atomic dipoles around the hydrogen bonds. It must be underlined here that this enhanced coupling cannot be represented by Coulomb interaction between atomic point charges and dipoles calculated in isolated fragments.

To estimate the induced effect on the D−A distance along the OH chains, we have finally relaxed the O−H interatomic distance in the complex. This distance undergoes a reduction of about 0.27 Å in the excited and relaxed [TTF$(H_2C{=}O)_2$]* complex compared to its value in the relaxed [TTF$(H_2C{=}O)_2$] one. A similar effect is expected with a CT of 0.8 e, corresponding to the ionic phase of TTF-CA, by a further strengthening of the hydrogen bond. However, this situation cannot be reproduced in our simplified complex. For a CT larger

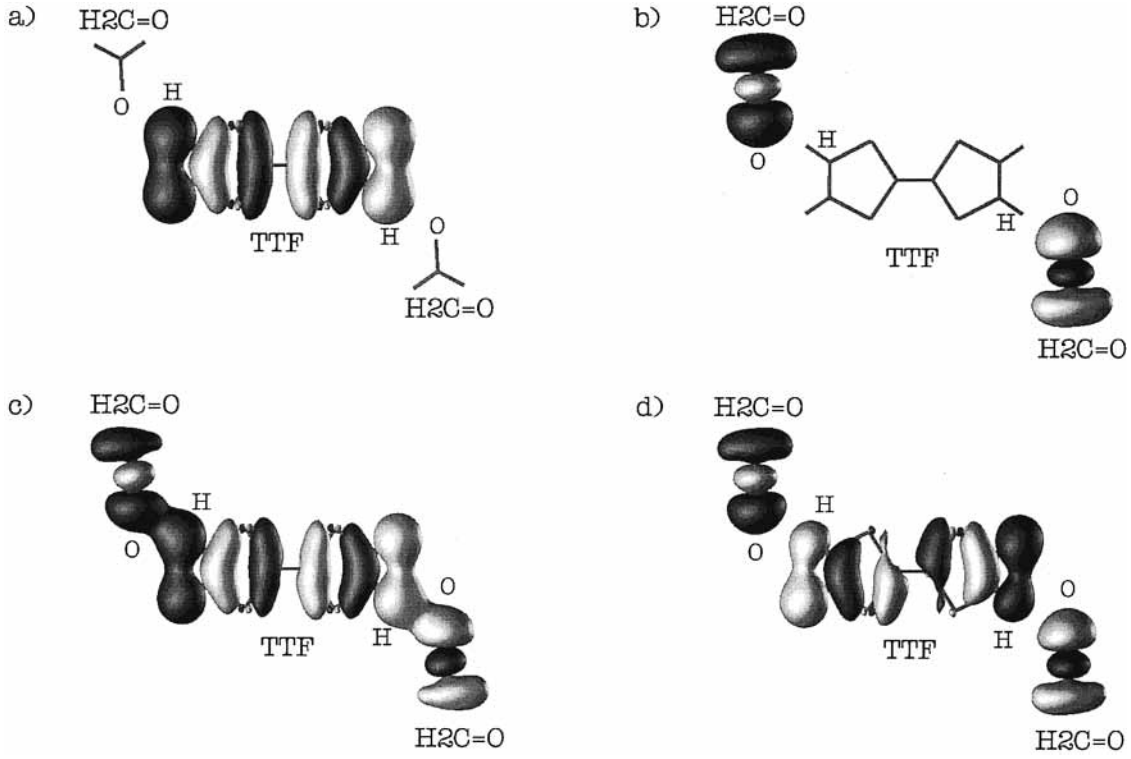

Figure 11. Example of bonding and antibonding hybridization between one MO of TTF and one MO of $(H_2C{=}O)_2$. Parts a and b represent, respectively, the MO's of the corresponding isolated fragments. Parts c and d represent the bonding and antibonding hybridizations in the complex (respectively, 8 eV and 7.6 eV below the HOMO).

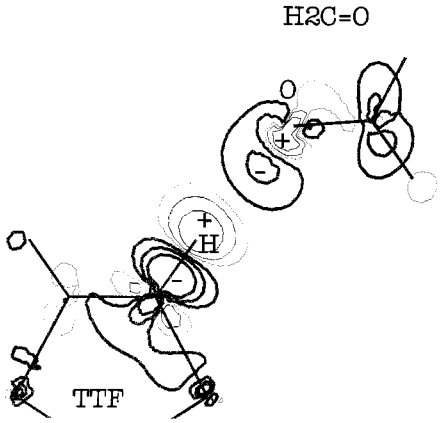

Figure 12. Isodensity curves of $\Delta n_P(\vec{r}) = n_{TTF(H_2C=O)_2}(\vec{r}) - n^0_{TTF}(\vec{r}) - n^0_{(H_2C=O)_2}(\vec{r})$ in the plane of the complex for ± 0.0005 e^-/au^3, ± 0.001 e^-/au^3, and ± 0.002 e^-/au^3.

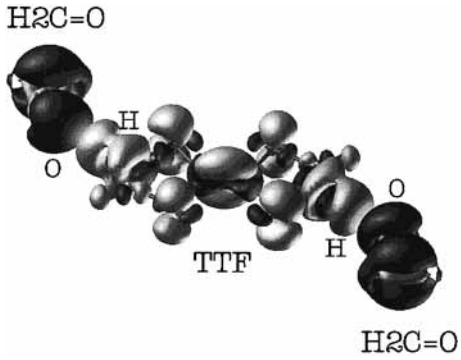

Figure 13. Isodensity representation $\Delta n^*(\vec{r}) = n_{[TTF(H_2C=O)_2]^*}(\vec{r}) - n^0_{TTF}(\vec{r}) - n^0_{(H_2C=O)_2}(\vec{r})$: dark (bright) isosurface corresponds to a gain (loss) of 0.0005 e^-/au^3.

than 0.5 e, the character of the LUMO of the complex is modified: the LUMO of $(H_2C{=}O)_2$ is shifted upward and is replaced by an empty state of TTF character. Nevertheless, the non-negligible shortening of the OH distance obtained here for a CT variation of 0.3 e compares well with its observed reduction of about 0.15 Å for CT variation of 0.5 e from the neutral phase at 300 K to the ionic phase at 40 K in TTF-CA.[1] In the crystal, a larger delocalization of the CT on the carbon ring of CA compared to its distribution on $H_2C{=}O$, together with steric hindrance effects, reduces the OH contraction. We have thus shown that the CT variation is related to the lattice contractions along the OH chains.

VI. Discussion

The uncommon N-I transition presented by some organic compounds are directly related to the peculiar molecular nature of these compounds. The N-I crystals are characterized by mixed stacks or "π chains" of D and A molecules and also by hydrogen bonds between coplanar D and A molecules along "OH chains". The corresponding electronic states are linear combinations of broad molecular orbitals, which can be deformed and polarized much easier than the individual atomic orbitals implicated in standard ferroelectric transitions observed, for example, in perovskites.

In each molecule, the MO's are coupled via repulsive electron−electron interactions, so that a charge variation in the frontier MO is associated, respectively, in A and D to a dilatation or a contraction of the electronic cloud of lower MO's, essentially in the molecular plane. This leaves an excess of charges of same sign on the periphery of each molecule and extra dipolar moments especially on O in A and H in D, thus increasing the reactivity of the molecules in their plane. This effect is enhanced in the crystals by the mutual influences of neighboring molecules.

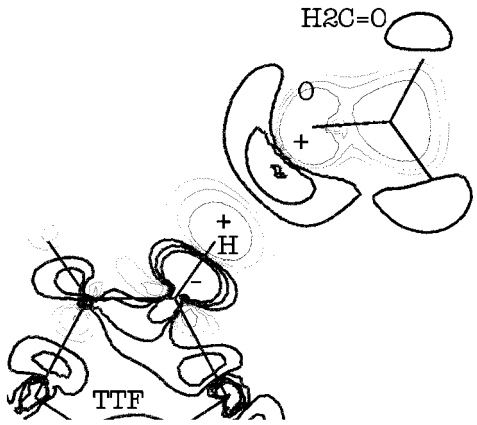

Figure 14. Isodensity curves of $\Delta n^*(\vec{r}) = n_{[TTF(H_2C=O)_2]^*}(\vec{r}) - n^0_{TTF}(\vec{r}) - n^0_{(H_2C=O)_2}(\vec{r})$ in the plane of the complex for ± 0.0005 e^-/au^3, ± 0.001 e^-/au^3, and ± 0.002 e^-/au^3.

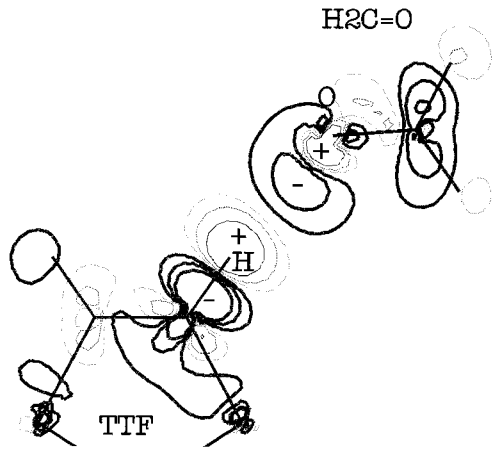

Figure 15. Isodensity curves of $\Delta n^*_P(\vec{r}) = n_{[TTF(H_2C=O)_2]^*}(\vec{r}) - n^{+0.3}_{TTF}(\vec{r}) - n^{-0.3}_{(H_2C=O)_2}(\vec{r})$ in the plane of the complex for ± 0.0005 e^-/au^3, ± 0.001 e^-/au^3, and ± 0.002 e^-/au^3.

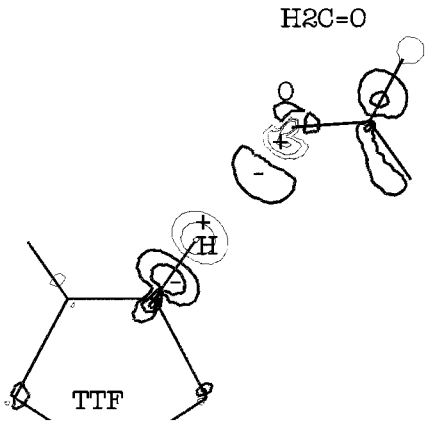

Figure 16. Isodensity curves of $\Delta n^*_P(\vec{r}) - \Delta n_P(\vec{r})$ in the plane of the complex for ± 0.0005 e^-/au^3, ± 0.001 e^-/au^3, and ± 0.002 e^-/au^3.

In the crystals, the electronic states in the vicinity of the Fermi level are of π character, so that the CT as well as some physical properties such as conductivity or optical properties are of nearly 1D character along the "π chains". The CT variation in the LS phase is directly related to a modification of the interaction between the frontier MO's of D and A, due to the molecular distortions and to the lattice contraction along the "π chains". But the ground state of the crystal and many features of its crystalline structure also rely on some deep intermolecular interactions, especially along the OH chains; we have shown that a CT variation induces a strengthening of these bonds and a lattice contraction along the OH chains. Hence the effects along the π and OH chains are intimately coupled in the CT and transition process.

This mechanism promotes the understanding of some aspects of the N-I transitions in the three compounds considered here. The intersecting π and OH chains form the crystallographic planes ($\vec{a}_1$, $\vec{a}_2$) in which all the molecules are in the same electronic state: either neutral or ionic, due to quantum nearest-neighbors contacts. For crystals where the interchain distances in the third direction $\vec{a}_3$ is relatively short, these chains are also strongly coupled in that direction by local electronic interactions, which favor a same electronic state. The transition to the I phase occurs hence simultaneously in all the chains. This is the case for TTF-CA and probably also for TTF-2,5Cl_2BQ, though only a few experimental data are available in this compound. In DMTTF-CA the intermolecular distances in the $\vec{a}_3$ direction are longer, so that the nearest-neighbor interactions in that direction are probably too weak to enforce a totally ionic configuration at low temperature. An intermediate N-I phase takes place,[3] characterized by a doubling of the unit cell in that direction and an alternation of N and I crystallographic planes.[10] A similar situation has also been encountered in an organic conductor[31] where a partial transition leads to a doubling of the unit cell and the appearance of two inequivalent BEDT-TTF molecules carrying different charges.

In this paper, we have revealed and analyzed a coupling between the CT variation and the anisotropic 3D lattice contractions via intramolecular electron−electron interactions between frontier and low-lying MO's. This mechanism plays an important part in the transitions under temperature or pressure variations, as well as in the cooperative relaxations accompanying photoexcitations in these compounds.[4] None of the terms considered up to now in models represent this mechanism. The analysis of the microscopic origin of the N-I transitions and their differences in different compounds necessitates to go beyond a two-band model, in a 3D scheme including a careful treatment of the hydrogen bonds.

This work has benefited from collaborations within the ψ_k-ESF Research Program and the Training and Mobility of Researchers Program "Electronic Structure" (Contract FMRX-CT98-0178) of the European Union. Parts of the calculations have been supported by the "Centre Informatique National de l'Enseignement Supérieur" (CINES-France). We thank P. E. Blöchl for his PAW code and H. Chermette and A. Boucekkine for useful discussions.

References and Notes

(1) Jacobsen, C. S.; Torrance, J. B. *J. Chem. Phys.* **1983**, *78*, 112. Mayerle, J. J.; Torrance, J. B.; Crowley, J. I. *Acta Crystallogr. B* **1979**, *35*, 2988.

(2) Brillante, A.; Girlando, A. *Phys. Rev. B* **1992**, *45*, 7026. Girlando, A.; Painelli, A.; Pecile, C.; Calestani, G.; Rizzoli, C.; Metzger, R. M. *J. Chem. Phys.* **1993**, *98*, 7692.

(3) Aoki, S.; Nakayama, T.; Miura, A. *Phys. Rev. B* **1993**, *48*, 626. Nogami, Y.; Taoda, M.; Oshima, K.; Aoki, S.; Nakayama, T.; Miura, A. *Synth. Met.* **1995**, *70*, 1219.

(4) Kikuchi, K.; Yakushi, K.; Kuroda, H. *Solid State Commun.* **1982**, *44*, 151. Okamoto, H.; Mitani, T.; Tokura, Y.; Koshihara, S.; Komatsu, K.; Iwasa, Y.; Koda, T. *Phys. Rev. B* **1991**, *43*, 8224.

(5) Nagaosa, N. *J. Phys. Soc. Jpn.* **1986**, *55*, 2754 and references therein. Painelli, A.; Girlando, A. *Phys. Rev. B* **1988**, *37*, 5748 and references therein.

(6) Nagaosa, N. *J. Phys. Soc. Jpn.* **1986**, *55*, 3488. Kojyo, N.; Onodera, Y. *J. Phys. Soc. Jpn.* **1987**, *56*, 3228.

(7) Girlando, A.; Pecile, C. *Solid State Commun.* **1985**, *54*, 753.

(8) LeCointe, M.; Lemée−Cailleau, M. H.; Cailleau, H.; Toudic, B.; Toupet, L.; Heger, G.; Moussa, F.; Schweiss, P.; Kraft, K. H.; Karl, N.

Phys. Rev. B **1995**, *51*, 3374. Lemée-Cailleau, M. H.; Le Cointe, M.; Cailleau, H.; Luty, T.; Moussa, F.; Roos, J.; Brinkmamn, D.; Toudic, B.; Ayache, C.; Karl, N. *Phys. Rev. Lett.* **1997**, *79*, 1690.

(9) Batail, P.; La Placa, S. J.; Mayerle, J. J.; Torrance, J. B. *J. Am. Chem. Soc.* **1981**, *103*, 951.

(10) Collet, E.; Buron−Le Cointe, M.; Lemée−Cailleau, M. H.; Cailleau, H.; Toupet, L.; Meven, M.; Mattauch, S.; Heger, G.; Karl, N. Manuscript in preparation.

(11) Katan, C.; Koenig, C.; Blöchl, P. E. *Solid State Commun*. **1997**, *102*, 589.

(12) Katan, C.; Koenig, C. *J. Phys.: Condens. Matter* **1999**, *11*, 4163.

(13) Blöchl, P. E. *Phys. Rev. B* **1994**, *50*, 17953.

(14) Car, R.; Parrinello, M. *Phys. Rev. Lett*. **1985**, *55*, 2471.

(15) Perdew, J. P.; Zunger, A. *Phys. Rev. B* **1981**, *23*, 5048.

(16) Ceperley, M.; Adler, B. L. *Phys. Rev. Lett.* **1980**, *45*, 566.

(17) Becke, A. D. *J. Chem. Phys.* **1992**, *96*, 2155.

(18) Perdew J. P. *Phys. Rev. B* **1986**, *33*, 8822.

(19) Nusterer, E.; Blöchl, P. E.; Schwarz, K. *Angew. Chem.* **1996**, *35*, 175. Nusterer, E.; Blöchl, P. E.; Schwarz, K. *Chem. Phys. Lett.* **1996**, *253*, 448.

(20) Blöchl, P. E. *J. Chem. Phys.* **1995**, *103*, 7422.

(21) $(\vec{a}_1,\vec{a}_2,\vec{a}_3) = (\vec{a},b,\vec{c})$ for TTF-CA, $(b,\vec{a},\vec{c})$ for TTF-2,5Cl_2BQ, and $(\vec{c},\vec{a},b)$ for DMTTF-CA. In TTF-CA, to each π or OH chain corresponds an equivalent π' or O′H′ chain in the direction $\vec{a}_2 - \vec{a}_1/2$, due to the existence of a glide plane perpendicular to $\vec{a}_2$.

(22) Coppens, P. *X-ray charge densities and chemical bonding*; International Union of Crystallography, Oxford University Press: Oxford, 1997.

(23) Katan, C.; Koenig, C.; Blöchl, P. E. *Comput. Mater. Sci.* **1998**, *10*, 325.

(24) Katan, C. *J. Phys. Chem. A* **1999**, *103*, 1407.

(25) Katan, C.; Blöchl, P. E.; Margl, P.; Koenig, C. *Phys. Rev. B* **1996**, *53*, 12112.

(26) Carloni, P.; Blöchl, P. E.; Parrinello, M. *J. Phys. Chem. A* **1995**, *99*, 1338.

(27) Green, D. C. *J. Org. Chem.* **1979**, *44*, 1476.

(28) Fukui, K. *Science* **1982**, *218*, 747.

(29) Chermette, H. *J. Comput. Chem.* **1999**, *20*, 129.

(30) Turi, L.; Dannenberg, J. J. *J. Phys. Chem.* **1993**, *97*, 7899. Espinosa, E.; Souhassou, M.; Lachekar, H.; Lecomte, C. *Acta Crystallogr. B* **1999**, *55*, 563.

(31) Guionneau, P.; Kepert, C. J.; Rosseinsky, M.; Chasseau, D.; Gaultier, J.; Kurmoo, M.; Hursthouse, M. B.; Day, P. *J. Mater. Chem.* **1998**, *8*, 367.